Understanding quantum interference in coherent molecular conduction

Gemma C. Solomon,[a] David Q. Andrews,[b] Thorsten Hansen, Randall H. Goldsmith,
Michael R. Wasielewski, Richard P. Van Duyne, and Mark A. Ratner
Department of Chemistry, Northwestern University, Evanston, Illinois 60208, USA

Theory and experiment examining electron transfer through molecules bound to electrodes are increasingly focused on quantities that are conceptually far removed from current chemical understanding. This presents challenges both for the design of interesting molecules for these devices and for the interpretation of experimental data by traditional chemical mechanisms. Here, the concept of electronic coupling from theories of intramolecular electron transfer is extended and applied in the scattering theory (Landauer) formalism. This yields a simple sum over independent channels, that is then used to interpret and explain the unusual features of junction transport through cross-conjugated molecules and the differences among benzene rings substituted at the ortho, meta, or para positions. © *2008 American Institute of Physics.* [DOI: 10.1063/1.2958275]

The past ten years have seen the development of techniques to measure the conductance of small numbers of molecules between electrodes, bringing a renewed challenge to understand the details of molecular junction electron transport. Much of today's qualitative understanding comes from the earlier work on intramolecular electron transfer (ET) and the theories of Marcus,[1] Marcus and Sutin,[2] and Hush.[3,4] The challenge faced today arises as the observable quantities (current, conductance, shot noise, etc.) are increasingly far removed from the chemical understanding that can be used in molecular design. This, in turn, limits the scope of the investigations of chemical space for finding promising molecules for electronic devices. The conductance characteristics of a large majority of molecules considered to date can be explained within the conventional coherent tunneling understanding; however, the unusual transmission characteristics of cross-conjugated molecules,[5] the unusual properties of benzene rings connected through the meta position,[6–12] and other calculations on larger structures[10,13–20] require extension of the simplest picture.

Here we take steps to redress this deficiency. We first examine how the transmission through molecules connected to electrodes can be separated into contributions from chemically familiar quantities. Then, second, how this understanding can be applied to model systems representing cross-conjugated molecules and benzene rings, to explain how interference effects come to dominate in those systems.

Chemical ET theory is replete with concepts that are useful both in explaining the ET properties and giving a chemical sense of the molecule involved. The first step in introducing chemical understanding to the descriptions of ET through molecules bound to electrodes is to show how these concepts map onto the methods used today. Previous work in this area has focused on showing the relationship between the rate based expression for electron transfer and the Land-

auer formula for the conductance through a molecular junction.[21,22] Here we introduce another tool for understanding molecular transport by extending the notion of coupling and applying it to junctions. The work of Marcus and Hush showed that for nonadiabatic intramolecular ET the transfer rate goes as the square of the electronic coupling between donor and acceptor; yet while there are a number of commonly used methods to calculate the coupling, they all present challenges.[23] To investigate this idea the first task is to find an expression for electronic coupling that can be applied to both donor-bridge-acceptor systems and electrode-molecule-electrode systems and, at the same time, connect this to the Landauer and scattering theory expressions for ET. Such an expression has already been examined in the context of scattering theory,[6,13] here we wish to continue from that work and derive similar results in the formal framework most commonly used in single molecule conduction calculations.

We start with the simplest form of the transmission[24–27] as given by

$$T(E) = \text{Tr}[\Gamma^L(E)G^r(E)\Gamma^R(E)G^a(E)], \qquad (1)$$

with $G^r(E)$ and $G^a(E)$ the retarded and advanced Green's functions of the molecule.

We can write the Γ_L and Γ_R matrices as

$$\Gamma_{ij}^L(E) = 2\pi \sum_\alpha V_{i\alpha}^L V_{\alpha j}^L \delta(E - \epsilon_\alpha^L),$$

$$\Gamma_{ij}^R(E) = 2\pi \sum_\beta V_{i\beta}^R V_{\beta j}^R \delta(E - \epsilon_\beta^R), \qquad (2)$$

where $V^{L(R)}$ are the coupling matrices connecting the electrodes (or donor and acceptor regions) with the molecule (or bridge). In this work the indices α and β are the indices of the left and right electrodes, respectively, and the indices i and j are the indices of the extended molecule component. Now we can define

[a] Electronic mail: g-solomon@northwestern.edu.
[b] Electronic mail: dqandrews@northwestern.edu.

$$d_{\alpha(\beta)}^{L(R)}(E) = \sqrt{2\pi\delta(E - \epsilon_{\alpha(\beta)}^{L(R)})}. \tag{3}$$

This is an unusual, yet well defined, quantity which we will show is useful for the manipulation of the equations. Then Γ^L and Γ^R reduce to

$$\Gamma_{ij}^L(E) = \sum_\alpha V_{i\alpha}^L d_\alpha^L(E) d_\alpha^L(E) V_{\alpha j}^L,$$

$$\Gamma_{ij}^R(E) = \sum_\beta V_{i\beta}^R d_\beta^R(E) d_\beta^R(E) V_{\beta j}^R. \tag{4}$$

From this we can rewrite Eq. (1) as

$$T(E) = \mathrm{Tr}[V^L d^L(E) d^L(E) V^{L^\dagger} G^r(E) V^R d^R(E) d^R(E) V^{R^\dagger} G^a(E)]. \tag{5}$$

The $\dagger$ denotes the conjugate transpose, or simply transpose in the case of real matrices. From here on $V^{L(R)}$ will occur with $d^{L(R)}$ so we can simplify the expressions by defining

$$\gamma^{L(R)}(E) = V^{L(R)} d^{L(R)}(E),$$

$$\gamma^{L(R)^\dagger}(E) = d^{L(R)}(E) V^{L(R)^\dagger}. \tag{6}$$

Equation (5) can then be rearranged using the equivalence of a trace to cyclic permutation and be expressed in its Hermitian form

$$\begin{aligned}
T(E) &= \mathrm{Tr}[(\gamma^{L^\dagger}(E) G^r(E) \gamma^R(E))(\gamma^{R^\dagger}(E) G^a(E) \gamma^L(E))] \\
&= \mathrm{Tr}[(\gamma^{L^\dagger}(E) G^r(E) \gamma^R(E))(\gamma^{L^\dagger}(E) G^r(E) \gamma^R(E))^\dagger] \\
&= \sum_{\alpha,\beta} \left| \sum_{i,j} \gamma_{\alpha,i}^{L^\dagger}(E) G_{i,j}^r(E) \gamma_{j,\beta}^R(E) \right|^2.
\end{aligned} \tag{7}$$

The advantage of writing the Hermitian form of the transmission in this way, instead of in terms of $\Gamma_{L(R)}^{1/2}$, is that it is clear where the electrode-molecule couplings remain in the expression and it allows for further simplification. This expression for the transmission can be converted to a formal rate expression for ET. This differs from standard ET rates because, following Datta[26] and Nitzan,[21] we assume that the effective state density for energy dissipation for an ET process in coherent junction transport is the electrode density of states appearing in Γ.

$$\begin{aligned}
k_{ET} &= \frac{1}{h} \int dE\, T(E) \\
&= \frac{2\pi}{\hbar} \int dE \sum_{\alpha,\beta} \left| \sum_{i,j} V_{\alpha,i}^{L^\dagger}(E) G_{i,j}^r(E) V_{j,\beta}^R(E) \right|^2 \\
&\quad \times \delta(E - \epsilon_\alpha^L) \delta(E - \epsilon_\beta^R) \\
&= \frac{2\pi}{\hbar} \sum_{\alpha,\beta} \left| \sum_{i,j} V_{\alpha,i}^{L^\dagger}(\epsilon_\alpha^L) G_{i,j}^r(\epsilon_\alpha^L) V_{j,\beta}^R(\epsilon_\alpha^L) \right|^2 \delta(\epsilon_\alpha^L - \epsilon_\beta^R) \\
&= \frac{2\pi}{\hbar} \sum_{\alpha,\beta} |t_{\alpha\beta}(\epsilon_\alpha^L)|^2 \delta(\epsilon_\alpha^L - \epsilon_\beta^R).
\end{aligned} \tag{8}$$

This is now a Golden rule-type expression for the rate of electron transfer, as given by scattering theory, derived from the Landauer equation. This permutation of the equation has

transformed the trace into a two-index sum over α and β (the electrode dimensions) and the dimension of the matrix under the trace is now left electrode by right electrode or equivalently donor by acceptor instead of the dimensions of the molecular block. This result is not striking in itself as the equivalence of these two approaches is well known; however, it is useful because in this form we can illuminate some other useful points.

The first point we can note is that the expression derived above for $t_{\alpha\beta}$ is equivalent to that derived earlier for the donor-acceptor coupling through the system.[28–31]

$$t_{\alpha\beta}^{DA}(E) = \sum_{i,j} V_{\alpha,i}^L G_{i,j}^r(E) V_{j,\beta}^R. \tag{9}$$

Conceptually, this provides a link between the Landauer–Imry equation, scattering theory and chemical electron transfer theory where it is understood that the electron transfer rate goes as the coupling through the bridging molecule squared. The coupling calculated by this method differs somewhat from convention because the inclusion of the self-energy in $G^r(E)$ results in the coupling being complex. If, instead of electrodes, we consider intramolecular ET the self-energies in $G^r(E)$ will not have a significant complex component and the coupling will more closely resemble its usual real form. This expression also provides a straightforward way to calculate the coupling through any extended system as the methods to calculate all the quantities in Eq. (9) are well established in the transport literature.[27,32–34]

The coupling and transmission through the molecule can be understood in terms of the contributions from different molecular conductance orbitals by a basis transformation. We can diagonalize G^r and G^a, with the overlap matrix S, and obtain the eigenvectors C_r and C_a.

$$G^{r'}(E) = C_r^{-1} S^{-1} G^r(E) C_r,$$

$$G^{a'}(E) = C_a^{-1} S^{-1} G^a(E) C_a = C_r^\dagger G^a(E) S^{-1} C_r^{-1\dagger}. \tag{10}$$

Molecular conductance orbitals differ from molecular orbitals in that by diagonalizing $G^r(E)$ instead of the Hamiltonian of the isolated molecule they may be complex; however, the molecular orbitals of the isolated molecule constitute their dominant component. As mentioned above, in the case of the complex coupling, in intramolecular electron transfer the nature of the self-energy will be such that the molecular conductance orbitals more closely resemble simple molecular orbitals than they will for a molecule bound to metallic electrodes.

The transmission [Eq. (7)] matrix can be transformed to give

$$\begin{aligned}
T(E) &= \mathrm{Tr}[\gamma^L(E) \gamma^{L^\dagger}(E) S C_r G^{r'}(E) C_r^{-1} \gamma^R(E) \\
&\quad \times \gamma^{R^\dagger}(E) S C_a G^{a'}(E) C_a^{-1}] \\
&= \mathrm{Tr}[\gamma^L(E) \gamma^{L^\dagger}(E) S C_r G^{r'}(E) C_r^{-1} \gamma^R(E) \gamma^{R^\dagger}(E) \\
&\quad \times (C_r^\dagger)^{-1} G^{a'}(E) C_r^\dagger S^{-1}].
\end{aligned} \tag{11}$$

This can be further simplified by defining some transformed matrices

$$\gamma^{L'}(E) = C_r^{\dagger} S^{-1} \gamma^{L}(E),$$

$$\gamma^{R'}(E) = C_r^{-1} \gamma^{R}(E). \tag{12}$$

Then Eq. (11) reduces to

$$T(E) = \mathrm{Tr}[\gamma^{L'^{\dagger}}(E) G^{r'}(E) \gamma^{R'}(E) \gamma^{R'^{\dagger}}(E) G^{a'}(E) \gamma^{L'}(E)]$$

$$= \mathrm{Tr}[(\gamma^{L'^{\dagger}}(E) G^{r'}(E) \gamma^{R'}(E))$$

$$\times (\gamma^{L'^{\dagger}}(E) G^{r'}(E) \gamma^{R'}(E))^{\dagger}]$$

$$= \sum_{\alpha,\beta} \sum_{i} |\gamma_{\alpha,i}^{L'^{\dagger}}(E) G_{i,i}^{r'}(E) \gamma_{i,\beta}^{R'}(E)|^2. \tag{13}$$

That is, we define the couplings, $t_{\alpha\beta}$, as

$$t_{\alpha\beta}(E) \equiv \sum_{i} V_{\alpha,i}^{L'^{\dagger}}(E) G_{i,i}^{r'}(E) V_{i,\beta}^{R'}(E), \tag{14}$$

where $V^{L(R)'}$ are transformed by the same transformations as $\gamma^{L(R)'}$. From this expression we can define a useful quantity $t_{\alpha\beta i} = V_{\alpha,i}^{L'^{\dagger}}(E) G_{i,i}^{r'}(E) V_{i,\beta}^{R'}$ which means that the coupling can then be written as

$$t_{\alpha\beta}(E) = \sum_{i} t_{\alpha\beta i}. \tag{15}$$

Now we have the result that the total transmission is given but the sum of contributions through each of the molecular conductance orbitals: each of the $t_{\alpha\beta}$ is given as a single index sum of the contributions ($t_{\alpha\beta i}$) from each of the eigenfunctions of G^r. Previous attempts to separate the transmission into contributions of individual molecular conductance orbitals failed to yield such a simple picture as the transmission was dominated by interference between pairs of orbitals.[35] Similarly, this expression provides a number of advantages for calculating coupling. Generally the donor/acceptor coupling is given by a series expansion; however, by diagonalizing G^r the series reduces to a single index sum. It should be noted that basis rotations that do not preserve the diagonal nature of $G^{r'}$ will result in the recovery of the two-index sum; consequently, the interpretation that follows is restricted to the case that $G^{r'}$ is diagonal. Through the use of this permutation of the equations the transmission and coupling through a molecule can be expressed as a sum of the contributions from each of the molecular conductance orbitals.

The transmission phase can be determined from the coupling, $t_{\alpha\beta}$

$$\theta_{\alpha\beta}(E) = \arctan[\mathrm{Im}(t_{\alpha\beta}(E))/\mathrm{Re}(t_{\alpha\beta}(E))]. \tag{16}$$

It is also possible to examine the phase of each of the constituent components of each $t_{\alpha\beta i}$

$$\theta_{\alpha\beta i}(E) = \arctan[\mathrm{Im}(t_{\alpha\beta i}(E))/\mathrm{Re}(t_{\alpha\beta i}(E))]. \tag{17}$$

We treat arctan as a multivalued function, continuously moving onto the next Riemann sheet each time the branch cut is passed. This then defines the phase of the transmission through each molecular conductance orbital as a function of energy. Note that, unlike $t_{\alpha\beta}$, in general, $\theta_{\alpha\beta}(E) \neq \Sigma_i \theta_{\alpha\beta i}(E)$.
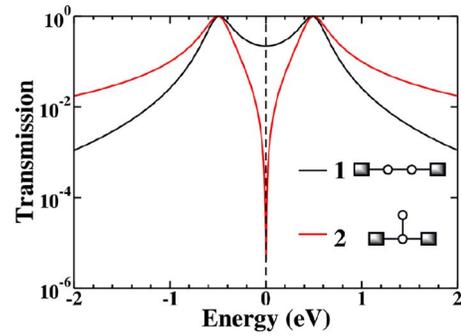

FIG. 1. (Color online) The transmission through the two two-site models.

As it is not obvious how to calculate $\gamma_{L(R)}$ in a simple fashion, we can proceed with our analysis using the scattering theory expression shown in Eq. (8) and substitute the transformed form of $t_{\alpha\beta}$ as shown in Eq. (14) in the place of $t_{\alpha\beta}$. We assume the wide band approximation (constant density of states) for our electrodes in all plots. We plot the total transmission through this system as $\Sigma_{\alpha,\beta} |t_{\alpha\beta}(E)|^2$, although in all the examples considered here there is only a single site binding.

The simplest system to illustrate the usefulness of the quantities discussed above is a two-site model system. In fact, we compare two model systems, the two-site model connected to the electrodes at each end (1) and the two-site model connected to both electrodes from the same site (2), illustrated in the inset to Fig. 1. The two-site model is described by a Hückel Hamiltonian

$$H_m = \begin{pmatrix} \alpha & \beta \\ \beta & \alpha \end{pmatrix}, \tag{18}$$

with site energies α and couplings β, these are set to 0 and -0.5, respectively. The single nonzero coupling element between the site and each electrode also set to -0.5.

Although these two models contain the same "molecule," their transmission characteristics differ considerably as shown in Fig. 1. The two systems have the same resonances; this is to be expected as the position of these largely correlates with the position of the molecular orbitals of the isolated molecule, which is obviously identical in these cases. However, the behavior on either side of the resonances differs. Above and below the energy of the resonances 2 has a higher transmission than 1, this can be understood as 2 has only one site in the transport direction whereas 1 has two. Between the resonances 2 has dramatically lower transmission than 1 due to the large interference feature at $E=0$. This is the model system which corresponds to the transmission behavior seen in branched structures[15,18,19] and cross-conjugated molecules.[36] This interference feature leads to unexpected consequences; particularly, it counters the conventional wisdom that transmission decreases with increasing bridge length. Importantly, the formalism introduced in the previous section provides the tools to understand how this occurs. The validity of the Landauer form of Eq. (1) is assumed in this work. When electron correlation on the molecule becomes important[37] this may fail, and so may our interpretation.
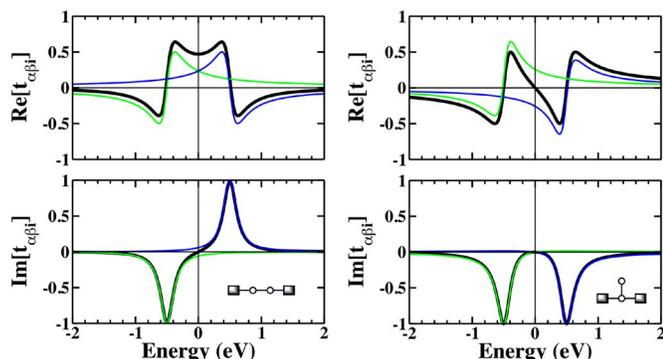
FIG. 2. (Color online) The contributions to the coupling from each molecular conductance orbital of the two two-site systems, 1 and 2 on the left and right, respectively. The contribution from the bonding orbital, the contribution from the antibonding orbital, and the sum of the two are shown. In the case of 2 both the real and imaginary components sum to zero at $E=0$ giving rise to the antiresonance in the transmission, recall that the energy eigenvalues of the parent orbitals are ± 0.5 eV.
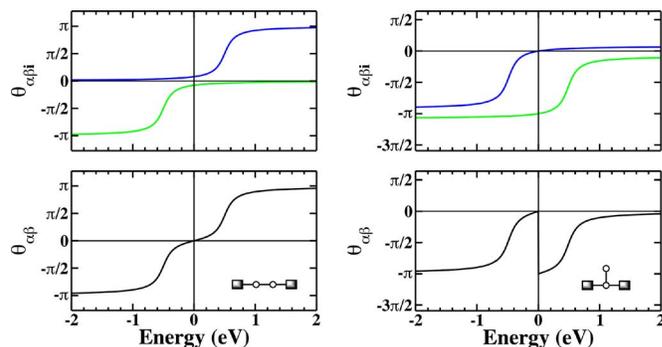
FIG. 3. (Color online) The phase of the transmission through each molecular conductance orbital (top) and the total phase of the transmission (bottom) for the two two-site systems. The total phase increases by π as the energy sweeps past a resonance and jumps discontinuously by π at the position of the antiresonance. At the antiresonance the phases through the molecular conductance orbital are separated by π leading to complete destructive interference. Note: in general, $\theta_{\alpha\beta}(E) \neq \Sigma_i \theta_{\alpha\beta i}(E)$.

It is now possible to separate the contributions to the transmission from each of the molecular conductance orbitals. These differ from molecular orbitals in that they may be complex; however, in the limit that electrode coupling goes to zero they become exactly the molecular orbitals. The influence of the electrode self-energies can be viewed as a perturbation and, consequently, the dominant contribution to the form of these conductance orbitals is known. We will refer to the bonding and antibonding molecular conductance orbitals which arise from the underlying bonding and antibonding molecular orbitals. The transmission through each molecular conductance orbital ($t_{\alpha\beta i}$) is shown in Fig. 2 for the two systems; they are complex quantities which are summed and squared to give the transmission as shown in Fig. 1. In this representation it is evident that the only difference between 1 and 2 is that the transmission through the antibonding orbital in 2 has a sign reversal compared to 1. It is striking that such a simple change to a single component in the transmission produces such dramatic results and, further, that this change is linked to a geometric change in the system.

The total coupling between the two electrodes, as mediated by the molecule, is given by the sum of the components illustrated in Fig. 2. In the case of 1 between the two resonances there is destructive interference in the minority, imaginary, component but constructive interference in the majority, real, component leading to nonzero coupling throughout the region. Conversely, in the case of 2 there is destructive interference in the dominant, real, component leading to the zero coupling between the resonances as the total coupling changes from positive to negative with increasing energy. While the sign of the coupling generally has little impact on the total transmission (which goes as coupling squared) it is clear that if the coupling components change sign it can have a significant impact as the total coupling may go through zero and a sharp interference feature will be seen.

The second component of the analysis that we can now perform is to examine the phase of the transmission through each molecular conductance orbital. It has previously been

noted in the scattering theory literature that the total phase of the transmission shifts steadily by π as the energy sweeps past a resonance and has a discontinuous jump of π at an antiresonance.[38] Figure 3 shows both the phase of the transmission through each molecular conductance orbital (top) and the total phase of the transmission (bottom). It is clear that the total transmission follows the pattern previously established, as the energy sweeps past each molecular resonance the phase increases by π and in the case of 2 there is a discontinuous jump of π at $E=0$, the position of the antiresonance.

The examination the phase of the transmission through each molecular conductance orbital provides additional information. Importantly, it is clear that at the position of the antiresonance in 2 the two coupling components through each orbital are precisely π out of phase. Together with the evidence from the coupling analysis, this is conceptually significant in understanding how this interference occurs and provides insight into what the two interfering paths are. The interfering paths, through the bonding and antibonding resonances, are not spatially separated. Both molecular orbitals are delocalized over both sites and the molecular conductance orbitals retain this form. This is similar to the result obtained by Lee[38] where the interfering paths were through even or odd parity quasibound states, and also to the result obtained by Sautet and Joachim,[6] in both cases there was no requirement for spatial separation of the paths. The physical sense of this result can be understood by considering the molecular analogs, linearly conjugated and cross-conjugated connection to an ethylene molecule. In that case, chemical understanding predicts that any electron in the π-system will be delocalized over both carbon atoms and interfering paths that are not spatially separated would concur with this understanding. This also has implications for understanding interference effects in benzene rings as we will discuss below. It had previously been suggested that different spatial paths through benzene might be responsible for the low transmission for the meta connected case;[10–12] however, this analysis shows that there may indeed be interference, yet it is not
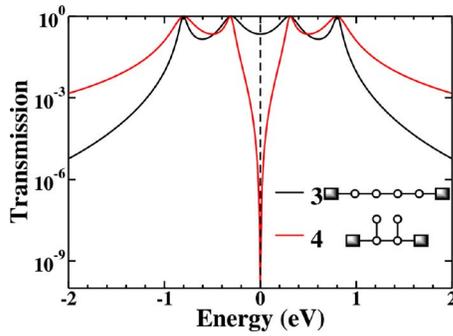
FIG. 4. (Color online) The total transmission through the two four-site models.

necessarily different spatial paths that are responsible as has also been suggested by previous work.[6,10]

Before turning our attention to cyclic systems it is worth noting how the results obtained above change with increasing system size. It is tempting to assume that interference between two energetically adjacent molecular conductance orbitals will occur at an energy between those orbitals; however, we will show that this is not always the case.

We consider two four-site models shown in the inset to Fig. 4, similar to the two-site models above, and examine how the transmission and phase features change. The transmission through these two models shown in Fig. 4 follows the same patterns, for similar reasons, to those outlined for the two-site models. The resonances are common to both models and the transmission above and below all the resonances is larger in the branched model due to the shorter chain in the transport direction. There is a strong interference feature in transmission for the branched model, 4, at $E=0$. It may seem unexpected that there is only a single antiresonance observed when there are now two side chains from the molecule. In fact, the antiresonance at $E=0$ is a degenerate pair of antiresonances which can be seen precisely by adding a small perturbation to the site energy of one of the side chain sites. Then, the antiresonances split and two can be observed. In the cases where an antiresonance arises from a single side chain site, the position of the antiresonance will be the site energy. If there are multiple single site side chains in a model the position of the antiresonances will only depend on their respective site energies.

The qualitative difference between the four-site models and the two-site models is in the energetic relationship between the interfering resonances. This can be seen by examining the coupling and the phase of the various components as shown in Figs. 5 and 6. The first striking difference between the four-site systems and the two-site systems is the remarkable similarity of the coupling and phase transmission through each of the molecular conductance orbitals for 3 and 4. It is only the result of differences in the relative widths of the contributions from each resonance that leads to complete destructive interference in the case of 4. Second, the orbital pairs which are π out of phase at $E=0$ are 1 with 3 and 2 with 4 (where we number the orbitals from lowest energy to highest energy resonance). Finally, the total phase transmission now has a jump of 2π at $E=0$ due to the two antiresonances. The total phase through 4 can be separated into two contributions from the sum of each of the pair orbitals.

$$\theta_{\alpha\beta1,3}(E) = \arctan[\mathrm{Im}(t_{\alpha\beta1}(E) + t_{\alpha\beta3}(E))/$$
$$\mathrm{Re}(t_{\alpha\beta1}(E) + t_{\alpha\beta3}(E)))],$$

$$\theta_{\alpha\beta2,4}(E) = \arctan[\mathrm{Im}(t_{\alpha\beta2}(E) + t_{\alpha\beta4}(E))/$$
$$\mathrm{Re}(t_{\alpha\beta2}(E) + t_{\alpha\beta4}(E)))].$$

(19)

In the lower panel of Fig. 6 $\theta_{\alpha\beta1,3}(E)$ is shown in green and $\theta_{\alpha\beta2,4}(E)$ in blue with the total phase through 4. These two combined contributions each take the same form as the total transmission phase of 2 and together sum to give the total transmission phase. In this way it is clear that the interference features in the transmission of 4 arise from interference between two sets of two interfering paths. The four-site systems also illustrate that interference may not always arise from interactions between energetically adjacent pairs of orbitals but that it can be understood in any case by an examination of the coupling and phase contributions.

It is instructive to examine in a little more detail the importance of the difference in the relative widths of the resonances between 3 and 4. The relative width of a resonance is controlled by how strongly the underlying orbital interacts with the electrodes, which, in turn, can be estimated by the magnitude of the orbital density at the sites closest to the electrodes (if the electrode binding site distance is fixed). In the case of 3, resonances 2 and 3 are wider than 1 and 4
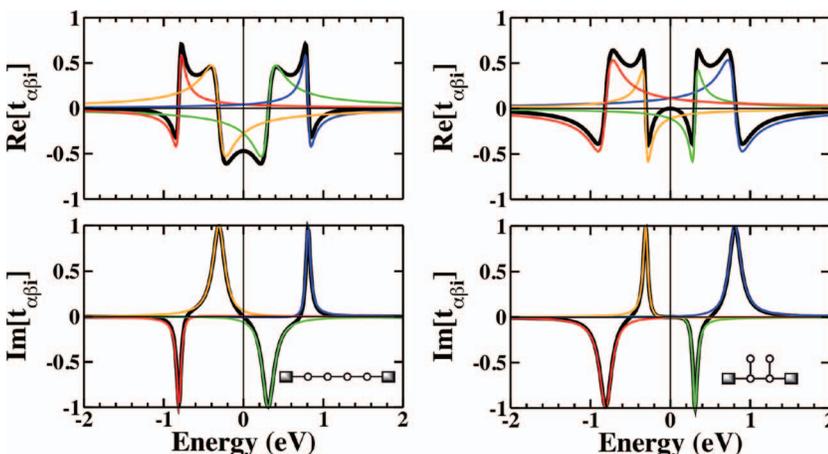

FIG. 5. (Color) The contributions to the coupling for the two four-site systems. In each case, the red, orange, green, and blue components are the contributions from each of the molecular conductance orbitals and the underlying black lines show the sum of all four contributions.
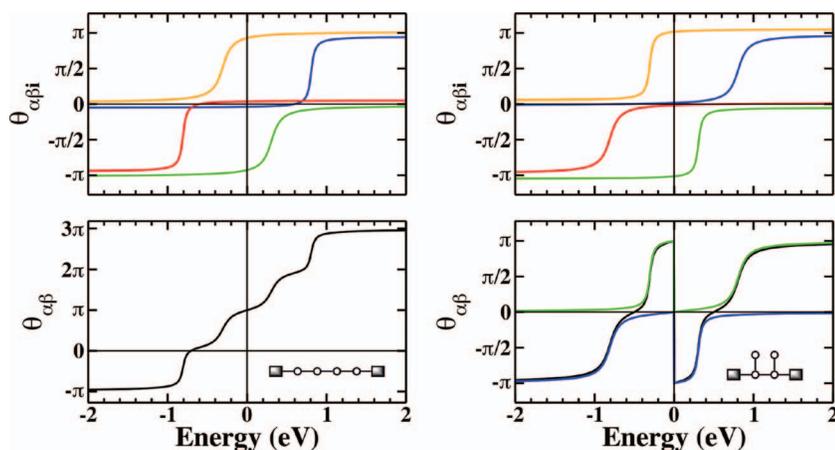
FIG. 6. (Color) The phase of the transmission through each molecular conductance orbital (top) and the total phase of the transmission (bottom) for the two four-site systems. Also shown for 4 in the lower panel are the transmission phases for the sum of the contributions from orbitals 1 and 3 (green) and 2 and 4 (blue), in each case there is jump of π at $E=0$ indicating the presence of the antiresonances.

resulting in their dominance of the total coupling at $E=0$. Conversely, it is the reversal of this pattern in 4 that allows all four terms to have equal weight at $E=0$ and the cancellation leading to the antiresonance. In recent work on interference[36] it is noted that systems where interference dominated were systems that could not be approximated with a simple barrier tunneling model, it is the relative width of the coupling terms that shows why this is the case. The general success in modeling molecular transmission[39] with a Simmons' model[40] was achieved under the assumption that the energetically proximate orbitals (in this case orbitals 2 and 3) would dominate at energies between them. It is clear that this is the case where the interference effects are minimal as in 3, but it is also clear that this assumption is problematic in the case of 4. It is interesting to note that this result shows that, in some cases, the width of the resonances can be used to determine whether a Simmons' model analysis will yield sensible results and in the case that energetically proximate resonances are narrower than energetically more distant ones it would indicate that this type of analysis will lead to erroneous conclusions.

The final example we consider is six-membered-ring models. These models differ in the manner by which they are connected to the electrodes. The three modes of connection considered mimic the ortho, meta, and para connections through a benzene ring. The model is shown schematically in Fig. 7.

Previous work, both experimental and theoretical,[7–11] has noted that the transmission through a benzene ring substituted at the meta position is dramatically lower than that through the ortho or para connections. Here, in Fig. 8 we illustrate this in the transmission close to the Fermi energy of the electrodes (here nominally at zero). In addition, we show that interference features similar to the one responsible for this difference are evident for the ortho connection; however, in that case they are further from the Fermi energy. It should be noted that only four resonances are apparent as the six-membered ring has two pairs of degenerate orbitals which underlie the middle two peaks in the transmission. In the para case one of each of the orbitals in the degenerate pairs does not contribute to the transmission. The very narrow interference features in both the ortho and meta transmissions around ±0.5 eV arise from the degeneracy breaking interactions with the electrodes and are not seen if the influence of the electrode (self-energies) are not included in Green's function.

An examination of the contributions of each of the molecular conductance orbitals to the coupling, Fig. 9, shows that majority of the antiresonance features in benzene do not arise from simple cancellation between the contributions of pairs of resonances. In fact, the only interference feature that does arise like this is the 0 eV feature in the meta case. All other features arise from more complicated combinations of canceling terms. Nonetheless, in all cases the cancellation can be predicted from an examination of the coupling and phase transmission through the system.

The six-membered ring systems show a combination of the effects seen in the previous two classes of systems. Here
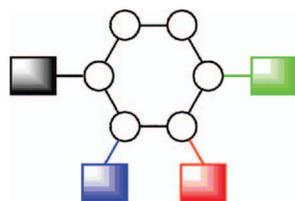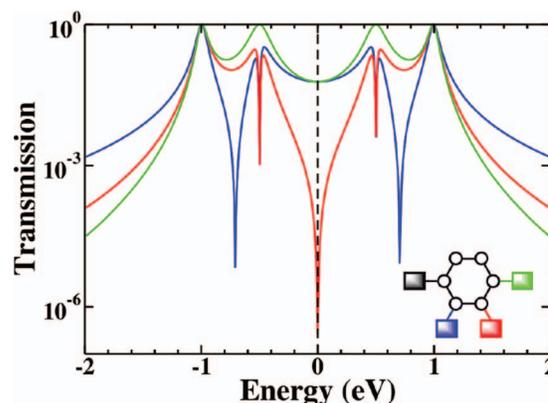

FIG. 7. (Color) The six-membered ring models. All models include the black electrode, the six-membered ring and one of the other electrodes, specifically the ortho, meta, and para connections use the blue, red, and green connections, respectively.

FIG. 8. (Color) The six-membered ring models. All models include the black electrode, the six-membered ring and one of the other electrodes, specifically the ortho, meta, and para connections use the blue, red, and green connections, respectively.
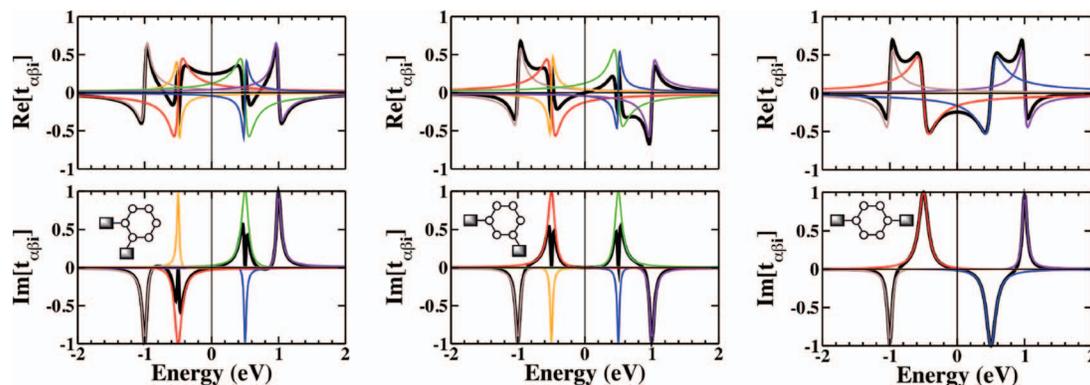
FIG. 9. (Color) The contributions to the coupling for the three six-membered ring systems with ortho, meta, and para connections to the electrodes shown on the left, middle, and right, respectively. The brown, red, orange, green, blue, and purple curves illustrate the contribution from each of the molecular conductance orbitals and the underlying black line gives the total in each case.

both the relative signs of the coupling terms and their relative widths are important in controlling which combination of contributions can interfere destructively and produce an antiresonance. As the complexity of the system considered increases the number and energetic relationship of the orbitals that interfere to produce antiresonances can also become increasingly complex; however, in all cases it is the sign and the width of these contributions that control their effects.

Together these results illustrate the way chemical concepts, in this case coupling, can provide the tools to dissect unexpected results. It is clear[21] that there are intimate links between scattering theory, the Landauer equation and intramolecular electron transfer theory and, in order to stimulate further progress, these links need to be elucidated. Extending the concept of coupling, allowing it to be separated into contributions from different molecular conductance orbitals, is a particularly powerful and intuitive link. Indeed, the idea that transmission could be separated into contributions from different resonances was pervasive, but had never been explicitly demonstrated.

Simple models to describe complex phenomena will always be attractive and it is important to be able to clearly see when such models will break down. This is illustrated here for the application of Simmons' barrier tunneling model to describe molecular conductance. The success of this model has been demonstrated (many instances, for example[39]) yet it is also clear that there are situations where it will break down;[5] here we demonstrate how simply examining the width of the resonances in a transmission spectrum can give an indication of why Simmons' model may be inappropriate in those cases.

The analysis of coupling and transmission phase through the model systems considered here provides useful information for a path-type picture of quantum interference in molecules. In particular, it can be shown that the interfering components arise from paths which, although orthogonal, are not necessarily spatially separated in terms of the atoms that participate. This presents a challenge for finding a classical analog for this interference, something reminiscent of a two-slit experiment. In some sense, it is not so surprising that classical analogs fail to describe quantum interference at the single molecule level; but the fact that they do, shows why

we need all the intuition we can get for these systems to understand and predict their behavior.

[1] R. Marcus, J. Chem. Phys. **24**, 966 (1956).
[2] R. Marcus and N. Sutin, Biochim. Biophys. Acta **811**, 265 (1985).
[3] N. Hush, Trans. Faraday Soc. **57**, 557 (1961).
[4] N. Hush, Electrochim. Acta **13**, 1005 (1968).
[5] G. C. Solomon, D. Q. Andrews, R. P. Van Duyne, and M. A. Ratner, J. Am. Chem. Soc. **130**, 7788 (2008).
[6] P. Sautet and C. Joachim, Chem. Phys. Lett. **153**, 511 (1988).
[7] C. Patoux, C. Coudret, J. P. Launay, C. Joachim, and A. Gourdon, Inorg. Chem. **36**, 5037 (1997).
[8] S. N. Yaliraki and M. A. Ratner, Ann. N. Y. Acad. Sci. **960**, 153 (2002).
[9] M. Mayor, H. B. Weher, J. Reichert, M. Elbing, C. von Hänisch, D. Beckmann, and M. Fischer, Angew. Chem., Int. Ed. **42**, 5834 (2003).
[10] D. Walter, D. Neuhauser, and R. Baer, Chem. Phys. **299**, 139 (2004).
[11] D. M. Cardamone, C. A. Stafford, and S. Mazumdar, Nano Lett. **6**, 2422 (2006).
[12] C. A. Stafford, D. M. Cardamone, and S. Mazumdar, Nanotechnology **18**, 424014 (2007).
[13] P. Sautet and C. Joachirn, Chem. Phys. **135**, 99 (1989).
[14] C. Joachim, J. K. Gimzewski, and H. Tang, Phys. Rev. B **58**, 16407 (1998).
[15] C. Kalyanaraman and D. G. Evans, Nano Lett. **2**, 437 (2002).
[16] R. Baer and D. Neuhauser, J. Am. Chem. Soc. **124**, 4200 (2002).
[17] S. Ami, M. Hliwa, and C. Joachim, Nanotechnology **14**, 283 (2003).
[18] R. Collepardo-Guevara, D. Walter, D. Neuhauser, and R. Baer, Chem. Phys. Lett. **393**, 367 (2004).
[19] M. Ernzerhof, M. Zhuang, and P. Rocheleau, J. Chem. Phys. **123**, 134704 (2005).
[20] I. Duchemin, N. Renaud, and C. Joachim, Chem. Phys. Lett. **452**, 269 (2008).
[21] A. Nitzan, J. Phys. Chem. A **105**, 2677 (2001).
[22] S. Yeganeh, M. A. Ratner, and V. Mujica, J. Chem. Phys. **126**, 161103 (2007).
[23] A. M. Kuznetsov and J. Ulstrup, *Electron Transfer in Chemistry and Biology* (Wiley, Chichester, UK, 1999).
[24] R. Landauer, IBM J. Res. Dev. **1**, 223 (1957).
[25] R. Landauer, Philos. Mag. **21**, 863 (1970).
[26] S. Datta, *Electronic Transport in Mesoscopic Systems* (Cambridge University Press, Cambridge, England, 1997).
[27] Y. Xue, S. Datta, and M. A. Ratner, Chem. Phys. **281**, 151 (2002).

[28] M. A. Ratner, J. Phys. Chem. **94**, 4877 (1990).
[29] J. N. Onuchic, P. C. P. de Anciracle, and D. N. Beratan, J. Chem. Phys. **95**, 1131 (1991).
[30] J. W. Evenson and M. Karplus, J. Chem. Phys. **96**, 5272 (1992).
[31] V. Mujica, M. Kemp, and M. A. Ratner, J. Chem. Phys. **101**, 6849 (1994).
[32] M. Brandbyge, J.-L. Mozos, P. Ordejón, J. Taylor, and K. Stokhro, Phys. Rev. B **65**, 165401 (2002).
[33] A. Pecchia and A. Di Carlo, Rep. Prog. Phys. **67**, 1497 (2004).
[34] F. Zahid, M. Paulsson, E. Polizzi, A. W. Ghosh, L. Sicldiqui, and S. Datta, J. Chem. Phys. **123**, 064707 (2005).
[35] G. C. Solomon, A. Gagliardi, A. Pecchia, T. Frauenheim, A. DiCarlo, J. R. Reimers, and N. S. Hush, Nano Lett. **6**, 2431 (2006).
[36] G. C. Solomon, D. Q. Andrews, R. H. Goldsmith, T. Hansen, M. R. Wasielewski, R. P. Van Duyne, and M. A. Ratner (unpublished).
[37] Y. Meir and N. Wingreen, Phys. Rev. Lett. **68**, 2512 (1992).
[38] H. W. Lee, Phys. Rev. Lett. **82**, 2358 (1999).
[39] H. B. Akkerman, R. C. G. Naber, B. Jongbloed, P. A. van Hal, P. W. M. Blom, D. M. de Leeuw, and B. de Boer, Proc. Natl. Acad. Sci. U.S.A. **104**, 11161 (2007).
[40] J. G. Simmons, J. Appl. Phys. **34**, 1793 (1963).